DOI 10.2478/ama-2023-0020

# FRACTIONAL ORDER, STATE SPACE MODEL OF THE TEMPERATURE FIELD IN THE PCB PLATE

**Krzysztof OPRZĘDKIEWICZ*, Wojciech MITKOWSKI*, Maciej ROSÓŁ***

*Faculty of Electrical Engineering Automatic Control Informatics and Biomedical Engineering,
Department of Automatic Control and Robotics, AGH University of Science and Technology,
al. A Mickiewicza 30, 30-059 Kraków, Poland

kop@agh.edu.pl, wojciech.mitkowski@agh.edu.pl, mr@agh.edu.pl

*received 9 July 2022, revised 26 October 2022, accepted 6 November 2022*

**Abstract:** In the paper the fractional order, state space model of a temperature field in a two-dimensional metallic surface is addressed. The proposed model is the two dimensional generalization of the one dimensional, fractional order, state space of model of the heat transfer process. It uses fractional derivatives along time and length. The proposed model assures better accuracy with lower order than models using integer order derivatives. Elementary properties of the proposed model are analysed. Theoretical results are experimentally verifed using data from industrial thermal camera.

**Key words:** fractional order systems, fractional order state equation, temperature field, heat transfer, thermal camera

Abbreviations: MIMO – Multiple Input Multiple Output, IO – Integer Order, FO – Fractional Order, CFE – Continuous Fraction Expansion, IIR – Infinite Impulse Response, FIR – Finite Impulse Response, PSE – Power Series Expansion.

## 1. INTRODUCTION

The modelling of processes and plants hard to describe using another mathematical tools is one of the main areas of application of the FO calculus.

Fractional models of different physical phenomena have been presented by many Authors for years. Fundamental results are presented e.g. by (1), (2) (the heating of an one dimensional beam), (3) (FO models of chaotic systems and Ionic Polymer Metal Composites), (4). Fractional Order diffusion processes are considered u.a. in (5), (6), (7). A collection of results using new Atangana-Baleanu operator can be found in (8). This book presents i.e. the FO blood alcohol model, the Christov diffusion equation and fractional advection-dispersion equation for groundwater transport processes.

Recently FO models are used u.a. to describe a spread of diseases. This issue is considered e.g. in the papers: (9) (the modelling of the dynamics of COVID using Caputo-Fabrizio operator), (10) (the modelling of a transmission of Zika virus using Atangana-Baleanu operator).

The state space FO models of the one dimensional heat transfer have been proposed in many previous papers of authors, e.g. (11), (12), (13), (14), (15), (16), (17), (18). These models employed different FO operators: Grünwald-Letnikov, Caputo, Caputo-Fabrizio and Atangana-Baleanu as well as discrete operators CFE and PSE. Each proposed model has been thoroughly theoretically and experimentally verified. In addition, each of them assures better accuracy in the sense of square cost function than its IO analogue.

Models of temperature fields obtained with the use of thermal cameras are presented e.g. by (19), (20). Analytical solution of the two-dimensional, IO heat transfer equation is presented in the paper (21). Numerical methods of solution of PDE-s can be found, e.g., in (22). Fractional Fourier integral operators are analyzed u.a. by (23). It is important to note that a significant part of known investigations deals only with a steady-state temperature elds with omitting their dynamics.

The paper (24) presents the generalization of FO models mentioned above to a two dimensional surface. It is important to note that in this paper the FO derivation only along the time is considered. The derivation along both space coordinates is described by the 2'nd order operator.

In this paper we propose and analyze a new, FO, state space model of heat transfer in a flat metallic surface. The model uses FO derivatives along time and space coordinates. Such an approach allows to obtain the better accuracy in the sense of a square cost function than model proposed previously. In addition, it is expected that satisfying accuracy will be achieved for relatively low order. Our knowledge shows that such a model has not been proposed yet. The proposed approach can be employed e.g. to modelling and reconstruction images from thermal cameras.

The paper is organized as follows. Preliminaries recall some basic ideas from fractional calculus, necessary to present results. Next the model using FO operator along the time is remembered. Furthermore its generalization applying FO operators along both time and space coordinates is presented and analyzed. Finally theoretical results are verified with the use of experimental data.

sciendo
DOI 10.2478/ama-2023-0020
acta mechanica et automatica, vol.17 no.2 (2023)
Special Issue "Modern Trends in Automation and Robotics in tribute to Professor Tadeusz Kaczorek"

## 2. PRELIMINARIES

At the beginning the non-integer order, integro-differential operator is presented (see e.g. (1), (4), (25), (26)).

**Definition 1** *(The elementary non integer order operator)* The non-integer order integro-differential operator is defined as follows:

$$ {}_aD_t^{\alpha} g(t) = \begin{cases} \frac{d^{\alpha} g(t)}{dt^{\alpha}} & \alpha > 0 \\ g(t) & \alpha = 0 \\ \int_a^t g(\tau)(d\tau)^{-\alpha} & \alpha < 0 \end{cases} \tag{1} $$

where a and t denote time limits for operator calculation, $\alpha \in \mathbb{R}$ denotes the non integer order of the operation.

Next an idea of complete Gamma Euler function is recalled (see for example (26)):

**Definition 2** *(The complete Gamma function)*

$$ \Gamma(x) = \int_0^{\infty} t^{x-1} e^{-t} dt \tag{2} $$

An idea of Mittag-Leffler function needs to be given next. It is a non-integer order generalization of exponential function et and it plays crucial role in the solution of a FO state equation. The two parameter Mittag-Leffler function is defined as follows:

**Definition 3** *(The two parameter Mittag-Leffler function)*

$$ E_{\alpha,\beta}(x) = \sum_{k=0}^{\infty} \frac{x^k}{\Gamma(k\alpha+\beta)} \tag{3} $$

For $\beta$ = 1 we obtain the one parameter Mittag-Leffler function:

**Definition 4** *(The one parameter Mittag-Leffler function)*

$$ E_{\alpha}(x) = \sum_{k=0}^{\infty} \frac{x^k}{\Gamma(k\alpha+1)} \tag{4} $$

The fractional order, integro-differential operator (1) is described by different definitions, given by Grünwald and Letnikov (GL definition), Riemann and Liouville (RL definition) and Caputo (C definition). Relations between Caputo and Riemann-Liouville, between Riemann-Liouville and Grünwald-Letnikov operators are given e.g. in (27), (4). Discrete versions of these operators are analysed with details in (28). The C definition has a simple interpretation of an initial condition (it is analogical as in integer order case) and intuitive Laplace transform. Additionally its value from a constant equals to zero, in contrast to e.g. RL definition. That's why in the further consideration the C definition will be used. It is recalled beneath.

**Definition 5** *(The Caputo definition of the FO operator)*

$$ {}_0^C D_t^{\alpha} f(t) = \frac{1}{\Gamma(V-\alpha)} \int_0^{\infty} \frac{f^{(V)}(\tau)}{(t-\tau)^{\alpha+1-V}} d\tau \tag{5} $$

In (5) $V$ is a limiter of the non-integer order: $V-1 \le \alpha < V$. If $V = 1$ then consequently $0 \le \alpha < 1$ is considered and the definition (5) takes the form:

$$ {}_0^C D_t^{\alpha} f(t) = \frac{1}{\Gamma(1-\alpha)} \int_0^{\infty} \frac{\dot{f}(\tau)}{(t-\tau)^{\alpha}} d\tau \tag{6} $$

Finally a fractional linear state equation using Caputo definition should be recalled. It is as follows:

$$ \begin{aligned} {}_0^C D_t^{\alpha} x(t) &= Ax(t) + Bu(t) \\ y(t) &= Cx(t) \end{aligned} \tag{7} $$

where $\alpha \in (0,1)$ is the fractional order of the state equation, $x(t) \in \mathbb{R}^R$, $u(t) \in \mathbb{R}^L$, $y(t) \in \mathbb{R}^P$ are the state, control and output vectors respectively, $A$, $B$, $C$ are the state, control, and output matrices.

## 3. THE EXPERIMENTAL SYSTEM AND ITS FO MODEL

The Figure 1 shows the simplified scheme of the considered heat system. This is the PCB plate of size $X \times Y$ pixels. The values of $X$ and $Y$ are determined by the resolution of a sensor of a camera. The plate is heated by at heater denoted by $H$. Its coordinates are denoted by $x_{h1}$, $x_{h2}$, $y_{h1}$ and $y_{h2}$ respectively. The surface area $S_H$ of the heater is equal:

$$ S_H = d_{xh} d_{yh} \tag{8} $$

where:

$$ \begin{aligned} d_{xh} &= x_{h2} - x_{h1} \\ d_{yh} &= y_{h2} - y_{h1} \end{aligned} \tag{9} $$

The temperature is measured using thermal camera, the area of measurement is configurable and denoted by $S$. Its coordinates are equal $x_{s1}$, $x_{s2}$, $y_{s1}$ and $y_{s2}$. The surface area $S_S$ of the measurement area is equal:

$$ S_S = d_{xs} d_{ys} \tag{10} $$

where:

$$ \begin{aligned} d_{xs} &= x_{s2} - x_{s1} \\ d_{ys} &= y_{s2} - y_{s1} \end{aligned} \tag{11} $$

More details about the construction of this laboratory system are given in the section "Experimental Results". The heat transfer in the surface is described by the Partial Differential Equation (PDE) of the parabolic type. All the side surfaces of plate are much smaller than its frontal surface. This allows to assume the homogeneous Neumann boundary conditions at all edges of the plate as well as the heat exchange on the surface needs to be also considered. It is expressed by coefficient $R_a$. The control and observation are distributed due to the size of heater and size of temperature eld read by camera. The heat conduction coefficient aw along both directions x and y is the same.

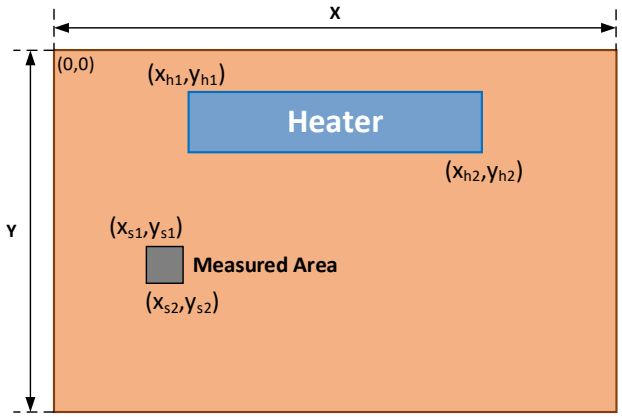


**Fig. 1.** The simplified scheme of the experimental system. Origin of the coordinate system is located in the left upper corner

DOI 10.2478/ama-2023-0020

The two dimensional, IO heat transfer equation has been considered in many papers (e.g. (29), (30), (31)). The fractional version with fractional derivative along the time and 2'nd order integer derivative along the length is presented with details in the paper (24).

This paper presents the model employing the fractional derivatives along both coordinates. This allows to obtain better accuracy with its smaller size.

The proposed model is as follows:

$$\begin{cases} {}_0^C D_t^\alpha Q(x,y,t) = a_w\left(\frac{\partial^\beta Q(x,y,t)}{\partial x^\beta} + \frac{\partial^\beta Q(x,y,t)}{\partial y^\beta}\right), \\ -R_a Q(x,y,t) + b(x,y)u(t), \\ \frac{\partial Q(0,y,t)}{\partial x} = 0, t \geq 0, \\ \frac{\partial Q(X,y,t)}{\partial x} = 0, t \geq 0, \\ \frac{\partial Q(x,0,t)}{\partial y} = 0, t \geq 0, \\ \frac{\partial Q(x,Y,t)}{\partial y} = 0, t \geq 0, \\ Q(x,y,0) = Q_0, 0 \leq x \leq X, 0 \leq y \leq Y, \\ y(t) = k_0 \int_0^X \int_0^Y Q(x,y,0)c(x,y)dxdy. \end{cases} \quad (12)$$

In (12) $\alpha$ and $\beta$ are non-integer orders of the system, $a_w > 0$, $R_a \in \mathbb{R}$ are coefficients of heat conduction and heat exchange, $k_0$ is a steady-state gain of the model, $b(x, y)$ and $c(x, y)$ are heater and sensor functions described as follows:

$$b(x,y) = \begin{cases} 1, x,y \in H \\ 0, x,y \notin H \end{cases} \quad (13)$$

$$c(x,y) = \begin{cases} 1, x,y \in S \\ 0, x,y \notin S \end{cases} \quad (14)$$

Let $\Omega \in \mathbb{R}^N$ it be an appropriate restricted area. The fractional Laplace operator $\Delta = \frac{\partial^\beta(..)}{\partial x^\beta} + \frac{\partial^\beta(..)}{\partial y^\beta}$ in $L^\beta(\Omega)$ with Dirichlet or Neumann boundary conditions is a discrete operator. The discrete operator has only a point spectrum (see e.g. (32), pp. 204, 460). Without going into details it is generally known from the spectral theorem for compact and self-adjoint operators that all eigenvalues $\lambda_{m,n}$ of the Laplace operator $\Delta$ in $L^2(\Omega)$ (with Dirichlet or Neumann boundary conditions) are non-negative, with finite multiplicities and $\lambda_n \to \infty$ for $n \to \infty$. Additionally, there is in $L^2(\Omega)$ an orthonormal basis (complete system) composed of eigenfunctions of the appropriate operator $\Delta$. In special cases of the area $\Omega \in \mathbb{R}^N$ (e.g. for a rectangle on a plane) analytical formulae for eigenvalues and eigenfunctions of the appropriate Laplace operator $\Delta$ can be given (see e.g. (33) pp. 21, 26 for the Dirichlet problem or (34) p 133, 138, 301, 305).

The Laplace operator $\Delta$ is self-adjointed, it has compact resolvent a it builds the Hilbert base $L^\beta(\Omega) = \{v: \int v^\beta(\xi)d\xi < \infty\}$ with standard scalar product $\langle v, u\rangle = \int_u u(\xi)y(\xi)d\xi$.

The eigenfunctions and eigenvalues for the Laplace operator $\Delta$ and Dirichlet boundary conditions are given u.a. by (34), pp.133, 138, 301, 305 or in book (32), pp.253-255.

The construction of the experimental system requires to assume the homogenous Neumann boundary conditions. This yields the following form of eigenfunctions and eigenvalues:

$$w_{m,n}(x,y) = \begin{cases} 1, m, n = 0, \\ \frac{2Y}{\pi n}\cos\frac{n\pi y}{Y}, m = 0, n = 1,2, \dots \\ \frac{2X}{\pi m}\cos\frac{m\pi x}{X}, n = 0, m = 1,2, \dots \\ \frac{2}{\pi}\frac{1}{\beta\sqrt{\frac{m^\beta}{X^\beta}+\frac{n^\beta}{Y^\beta}}}\cos\frac{m\pi x}{X}\cos\frac{n\pi y}{Y}, m,n = 1,2, \dots \end{cases} \quad (15)$$

$$\lambda_{m,n}(x,y) = -a_w\left[\frac{m^\beta}{X^\beta} + \frac{n^\beta}{Y^\beta}\right]\pi^\beta - R_a,\ m,n = 1,2, \dots \quad (16)$$

Consequently the considered two dimensional heat equation (12) can be expressed as an infinite dimensional state equation:

$$\begin{aligned} {}_0^C D_t^\alpha Q(t) &= AQ(t) + Bu(t) \\ y(t) &= CQ(t) \end{aligned} \quad (17)$$

where:

$$\begin{aligned} &AQ = a_w\left(\frac{\partial^\beta Q(x,y)}{\partial x^\beta} + \frac{\partial^\beta Q(x,y)}{\partial y^\beta}\right) - R_a Q(x,y), \\ &D(A) = \{Q \in H^2(0,1): Q'(0) = 0, Q'(X) = 0, Q'(Y) = 0\}, \\ &a_w, R_a > 0, \\ &CQ(t) = \langle c, Q(t)\rangle, Bu(t) = bu(t). \end{aligned} \quad (18)$$

The state vector $Q(t)$ is defined as beneath:

$$Q(t) = \left[q_{0,0}, q_{0,1}, q_{0,2}, \dots, q_{1,0}, q_{1,1}, q_{1,2}, \dots\right]^T \quad (19)$$

The main difference to the model presented in the paper (24) is that the non-integer order $\beta$ must be taken into account in the state, control and observation operators. This is presented below.

The state operator $A$ takes the following form:

$$A = diag\{\lambda_{0,0}, \lambda_{0,1}, \lambda_{0,2}, \dots, \lambda_{1,0}, \lambda_{1,1}, \dots, \lambda_{2,2}, \dots, , \lambda_{m,n}, \dots\}. \quad (20)$$

The control operator takes the following form:

$$B = \left[b_{0,0}, b_{0,1}, b_{0,2}, \dots, b_{1,0}, b_{1,1}, \dots\right]^T. \quad (21)$$

$$b_{m,n} = \langle H, w_{m,n}\rangle = \int_0^X \int_0^Y b(x,y)w_{m,n}(x,y)dxdy. \quad (22)$$

Taking into account (15) we obtain:

$$b_{m,n} = \begin{cases} S_H, m, n = 0, \\ \frac{2Y^2}{h_{yn}^2}d_{xh}a_{nhy}, m = 0, n = 1,2, \dots \\ \frac{2X^2}{h_{xm}^2}d_{yh}a_{mhx}, n = 0, m = 1,2, \dots \\ \frac{k_{mn}}{h_{xm}h_{yn}}a_{mhx}a_{nhy}, m,n = 1,2, \dots \end{cases} \quad (23)$$

where $S_H$, $d_{xh}$ and $d_{yh}$ are described by (8), (9) and:

$$\begin{aligned} h_{xm} &= \frac{m\pi}{X}, \\ h_{yn} &= \frac{n\pi}{Y}. \end{aligned} \quad (24)$$

$$k_{mn} = \frac{2}{\pi}\frac{1}{\beta\sqrt{\frac{m^\beta}{X^\beta}+\frac{n^\beta}{Y^\beta}}}. \quad (25)$$

$$\begin{aligned} a_{mhx} &= \sin(\mathbb{I}_{xm}x_{\mathbb{I}2}) - \sin(\mathbb{I}_{xm}x_{\mathbb{I}1}), \\ a_{nhy} &= \sin(\mathbb{I}_{yn}y_{\mathbb{I}2}) - \sin(\mathbb{I}_{yn}y_{\mathbb{I}1}). \end{aligned} \quad (26)$$

sciendo
DOI 10.2478/ama-2023-0020
acta mechanica et automatica, vol.17 no.2 (2023)
Special Issue "Modern Trends in Automation and Robotics in tribute to Professor Tadeusz Kaczorek"

The output operator is as beneath:

$$C = [c_{0,0}, c_{0,1}, c_{0,2}, \dots, c_{1,0}, c_{1,1}, \dots]. \quad (27)$$

where:

$$c_{m,n} = \langle S, w_{m,n} \rangle = \int_0^X \int_0^Y c(x,y) w_{m,n}(x,y) dxdy. \quad (28)$$

In (28) each element $c_{m,n}$ is expressed analogically, as (23):

$$c_{m,n} = \begin{cases} S_s, m, n = 0, \\ \frac{2Y^2}{h_{yn}^2} d_{xs} a_{nsy}, m = 0, n = 1,2, \dots \\ \frac{2X^2}{h_{xm}^2} d_{ys} a_{msx}, n = 0, m = 1,2, \dots \\ \frac{k_{mn}}{h_{xm} h_{yn}} a_{msx} a_{nsy}, m, n = 1,2, \dots \end{cases} \quad (29)$$

In (29) $h_{xm,yn}$ and $k_{mn}$ are expressed by (24), (25), $S_H$, $d_{xh}$ and $d_{yh}$ are described by (10), (11) and:

$$a_{msx} = \sin(\square_{xm} x_{s2}) - \sin(\square_{xm} x_{s1}), \quad a_{nsy} = \sin(\square_{yn} y_{s2}) - \sin(\square_{yn} y_{s1}). \quad (30)$$

### 3.1. The decomposition of the model

The decomposition of the model is done by the similar way as for the system considered in the paper (24). Due to the form of the state operator $A$ (20) the system (17)-(29) can be splitted to infinite number of independent scalar subsystems associated to particular eigenvalues:

$$D^\alpha Q(t) = AQ(t) + Bu(t),$$
$$Aw_{m,n} = \lambda_{m,n} w_{m,n}.$$
$$D^\alpha Q(t) = a_w \left( \frac{\partial^\beta Q}{\partial x^\beta} + \frac{\partial^\beta Q}{\partial y^\beta} \right) - R_a Q + Bu,$$
$$D^\alpha \sum_{m=0}^\infty \sum_{n=0}^\infty q_{m,n} = a_w \left( \sum_{m=0}^\infty \frac{\partial^\beta q_{m,n}}{\partial x^\beta} + \sum_{n=0}^\infty \frac{\partial^\beta q_{m,n}}{\partial y^\beta} \right) - -R_a \sum_{m=0}^\infty \sum_{n=0}^\infty q_{m,n} + Bu,$$
$$D^\alpha q_{m,n} = a_w \left( \frac{\partial^\beta q_{m,n}}{\partial x^\beta} + \frac{\partial^\beta q_{m,n}}{\partial y^\beta} \right) - R_a q_{m,n} + b_{m,n} u. \quad (31)$$

The form of equation (31) implies the decomposition of the system (7) into systems related to single eigenvalues $\lambda_{m,n}, m, n = 0,1,2, \dots$. This decomposition allows to easily compute the step and impulse responses of the system as a sum of responses of particular modes. This is presented below.

Assume the homogenous initial condition in the equation (12): $Q(x; y_0) = 0$. Then the step response is as follows:

$$y_\infty(t) = \sum_{m=1}^\infty \sum_{n=1}^\infty y_{m,n}(t). \quad (32)$$

where $m$, $n$-th mode of response is as follows:

$$y_{m,n}(t) = \frac{E_\alpha(\lambda_{m,n} t^\alpha) - 1(t)}{\lambda_{m,n}} b_{m,n} c_{m,n}. \quad (33)$$

In (33) $E_\alpha(..)$ is the one parameter Mittag-Leffler function (4), $\lambda_{m,n}$, $b_{m,n}$ and $c_{m,n}$ are expressed by (16), (22) and (28) respectively.

Analogically the impulse response takes the following form:

$$g_\infty(t) = \sum_{m=1}^\infty \sum_{n=1}^\infty g_{m,n}(t). \quad (34)$$

where $m$, $n$-th mode of response is as follows:

$$g_{m,n}(t) = E_{\alpha,\alpha}(\lambda_{m,n} t^\alpha) b_{m,n} c_{m,n}. \quad (35)$$

In (35) $E_{\alpha,\alpha}(..)$ is the two parameters Mittag-Leffler function (3).

During simulations it is possible to use of the finite - dimensional sums only. Consequently (32) and (34) take the following form:

$$y_{M,N}(t) = \sum_{m=0}^M \sum_{n=0}^N y_{m,n}(t). \quad (36)$$

$$g_{M,N}(t) = \sum_{m=0}^M \sum_{n=0}^N g_{m,n}(t). \quad (37)$$

The values of $M$ and $N$ assuring the assumed accuracy and convergence of the model can be estimated numerically or analytically.

### 3.2. The convergence

The convergence of the proposed model can be estimated using Rate of Convergence (ROC) defined as the steady-state value of the strongest damped mode of the step response. The estimation of it in the one dimensional case was relatively simple due to particular modes of a step response are in descending order.

In the two dimensional case particular modes of a step response are not ordered. In addition, eigenvalues (16) can be multiple. This makes the analysis of the convergence of the proposed model a little bit more complicated. The ROC is defined as follows:

$$ROC_{M,N} = \min_{M,N} \left| \frac{b_{M,N} c_{M,N}}{\lambda_{M,N}} \right|. \quad (38)$$

The relation (38) can be employed to numerical analysis of convergence in different places of measurement. This will be presented in the next section.

## 4. EXPERIMENTAL VALIDATION OF RESULTS

### 4.1. The experiments

Experiments were done with the use of the heat system shown in the Figure 2. The dimensions of the PCB plate in pixels are: $X$ = 380, $Y$ = 290. The PCB is heated by the heater 170x20 pixels with maximum power 10W located in points: $x_{h1}$ = 100, $y_{h1}$ = 40 The temperature field is read using thermal camera OPTRIS PI 450, connected to computer via USB and installed dedicated software OPTRIS PI CONNECT. The measured temperature covers range 0 – 250 °C, the sampling frequency is 80 Hz. The signal powering the heater is given from computer using NI LabView, NI myRIO and amplifier. The maximum current from amplifier equal 400mA at a voltage of 12V gives the maximum power 4:8W. The tested PCB plate is not isolated from the environment. This implies that measurements strongly depend on ambient temperature. An another cause of noise during The considered experiment was done in hot summer. During experiments the step response of the system was investigated. The "zero" level denotes the heater switched off, the "one" level is the full power of the heater.

DOI 10.2478/ama-2023-0020

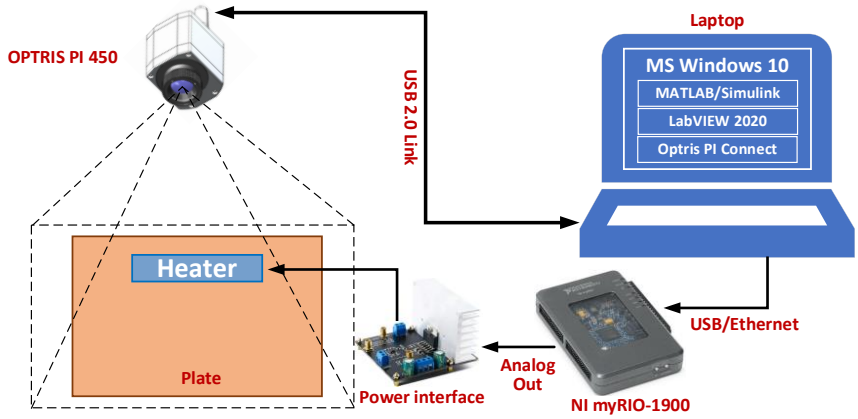


**Fig. 2.** The experimental system

The temperature fields for both states are shown in the Figure 3. This figure shows also the points of measurement of the step response, marked as "Area 1–4". Areas 1–3 are located in different points of plate, area 4 covers the heater and it describes its mean temperature. Coordinates of all measuring areas are described by the Table 1. The step responses in the selected areas 1, 2, 3 and 4 are shown in the Figure 4. During calculations these coordinates *x*.. and *y*.. were given relative to *X* and *Y*. For example, xs1 = 75 during calculating elements of C matrix with respect to (29) was equal: $x_{s1}$ = 75/380 = 0.1974.

**Tab. 1.** Coordinates of measuring areas (in pixels)

| Area | $x_{s1}$ | $y_{s1}$ | $x_{s2}$ | $y_{s2}$ |
|---|---|---|---|---|
| 1 | 50 | 75 | 52 | 77 |
| 2 | 200 | 100 | 202 | 102 |
| 3 | 300 | 200 | 302 | 202 |
| 4 | 120 | 40 | 250 | 60 |

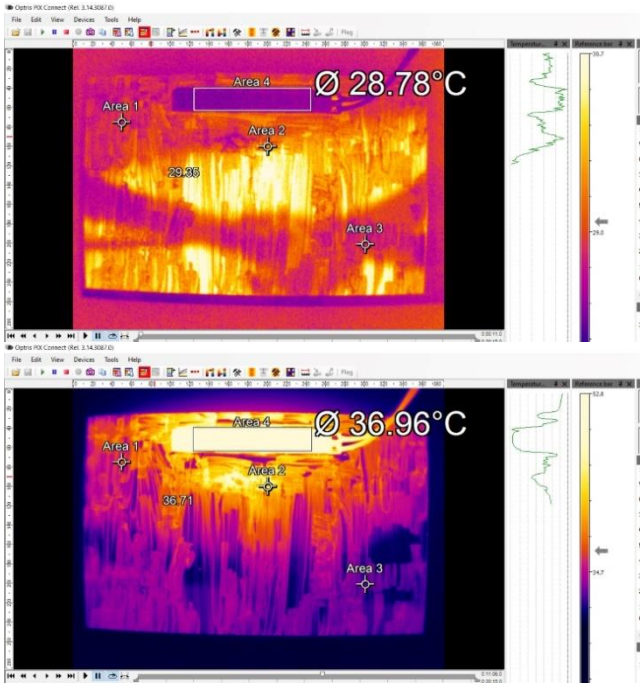


**Fig. 3.** The steady-state temperature fields for non-heated (top) and heated plate (bottom). The temperature strongly depends on ambient temperature. The colour scale in each case is different

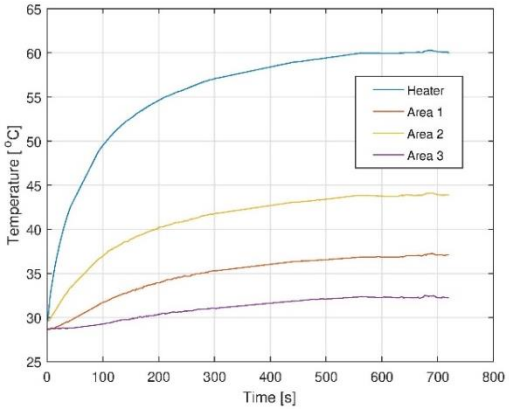


**Fig. 4.** The step responses of temperature in all tested fields

### 4.2. The identification of the model

The identification of parameters of the proposed model has been done via minimization of the Mean Square Error (MSE) cost function. This function describes the mean difference between the step responses of the plant and the model at the same time-spatial mesh:

$$MSE = \frac{1}{K}\sum_{k=1}^{K}[y(k) - y_e(k)]^2 \qquad (39)$$

In (39) *K* is the number of all collected samples, *y*(*k*) is the step response of the model, computed using (36), $y_e(k)$ is the experimental response measured in the same place and at the same time instants *k* with the use of thermal camera. The sample time during a step response measurement was equal 1[s]. In each case the mean temperature of the whole area is measured.

The cost function (39) is a function of parameters $\alpha$, $\beta$, $a_w$ and $R_a$. Its optimization was done with the use of the MATLAB function *fminsearch*, the step response was calculated using finite-dimensional formula (36). Calculations were done using the following values of both orders: *M* = *N* = 3 and *M* = *N* = 5.

Results are given in the tables 2. The comparison of step responses model vs experiment for M = N = 5 is presented in the Figure 5.

The results in tables 2 and 3 show that the use of 3'rd order model assures practically the same accuracy in the sense of cost function (39) as the use of 5'th order model. This result is confirmed by the convergence analysis presented in the next subsection.

sciendo
DOI 10.2478/ama-2023-0020
acta mechanica et automatica, vol.17 no.2 (2023)
Special Issue "Modern Trends in Automation and Robotics in tribute to Professor Tadeusz Kaczorek"

Next, if we recall the results from paper (24), the accuracy of the proposed model is practically the same as the accuracy of 8'th order model with integer order $\beta = 2$.

Tables 4 and 5 compare the values of cost function (39) for all considered models: integer order, fractional order along the time and fractional order along both coordinates.

**Tab. 2.** Identified parameters of the model for $M = N = 3$

| Area | $\alpha$ | $\beta$ | $a_w$ | $R_a$ | MSE (39) |
|---|---|---|---|---|---|
| 1 | 1.0794 | 1.8138 | 0.0033 | 0.0032 | 0.0110 |
| 2 | 0.9356 | 1.6167 | 0.0538 | 0.0089 | 0.0217 |
| 3 | 1.4878 | 1.8712 | 0.0208 | 0.0003 | 0.0059 |
| 4 | 0.8156 | 2.0028 | 0.0100 | 0.0235 | 0.0627 |

**Tab. 3.** Identified parameters of the model for $M = N = 5$

| Area | $\alpha$ | $\beta$ | $a_w$ | $R_a$ | MSE (39) |
|---|---|---|---|---|---|
| 1 | 1.0794 | 1.8641 | 0.0032 | 0.0032 | 0.0110 |
| 2 | 0.9590 | 0.3959 | 0.0357 | 0.0057 | 0.0207 |
| 3 | 1.4877 | 1.8712 | 0.0208 | 0.0003 | 0.0059 |
| 4 | 0.8156 | 1.2400 | 0.0098 | 0.0234 | 0.0627 |

**Tab. 4.** The cost function MSE for all models and $M = N = 3$

| Area | $\alpha = 2, \beta = 2$ | $\alpha \in \mathbb{R}, \beta = 2$ | $\alpha \in \mathbb{R}, \beta \in \mathbb{R}$ |
|---|---|---|---|
| 1 | 0.0233 | 0.0170 | 0.0110 |
| 2 | 0.0183 | 0.0205 | 0.0217 |
| 3 | 0.0644 | 0.1429 | 0.0059 |
| 4 | 1.1448 | 0.1145 | 0.0627 |

**Tab. 5.** The cost function MSE for all models and $M = N = 5$

| Area | $\alpha = 2, \beta = 2$ | $\alpha \in \mathbb{R}, \beta = 2$ | $\alpha \in \mathbb{R}, \beta \in \mathbb{R}$ |
|---|---|---|---|
| 1 | 0.0233 | 0.0170 | 0.0110 |
| 2 | 0.0497 | 0.0205 | 0.0207 |
| 3 | 0.0665 | 0.1162 | 0.0059 |
| 4 | 0.0920 | 0.1145 | 0.0627 |

Quite surprising is the large dispersion of values in the model parameters for points 1, 2 and 3, which are the same in terms of the material. This is probably caused by measurement disturbances related to light reflections and different emissivity of the surface.

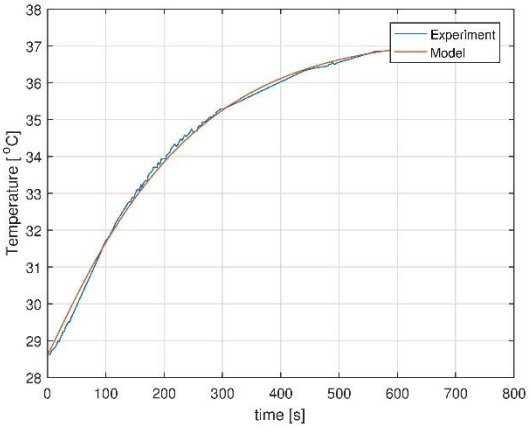


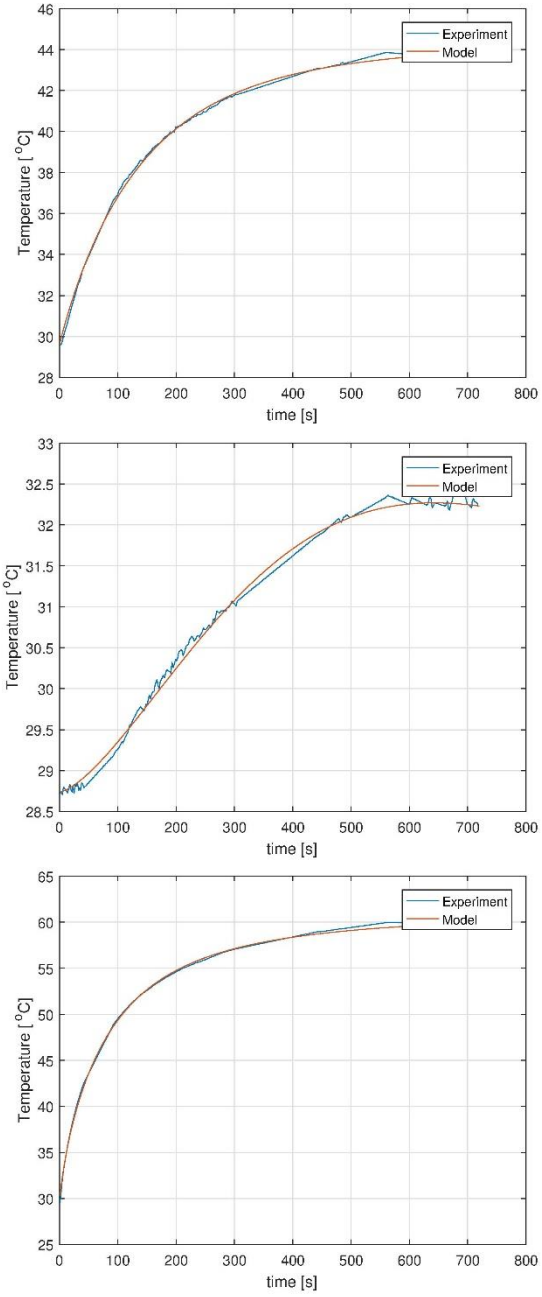


**Fig. 5.** The step responses of the FO model ($M = N = 5$) vs real plant for area 1(top) to 4 (bottom)

### 4.3. The numerical analysis of the convergence

The convergence of the proposed model can be estimated using the ROC coefficient expressed by (38). It is a function of place of measurement and a function of both orders of the model $M$ and $N$. However to simplify the analysis assume that both orders are equal: $M = N$. The value of ROC as a function of order $N$ for all tested places and for parameters given in the table 3 is presented in the Figure 38. From diagrams presented in Figure 38 it can be concluded that the maximum orders $M = N = 4$ assure the good accuracy of the model. Further increasing of orders does not improve the accuracy and increases computational complexity. This is compliant to results of identification, given in the tables 2-5. Next, the ROC depends not only on order $N$, but also on the location and size of place of measurement.

DOI 10.2478/ama-2023-0020

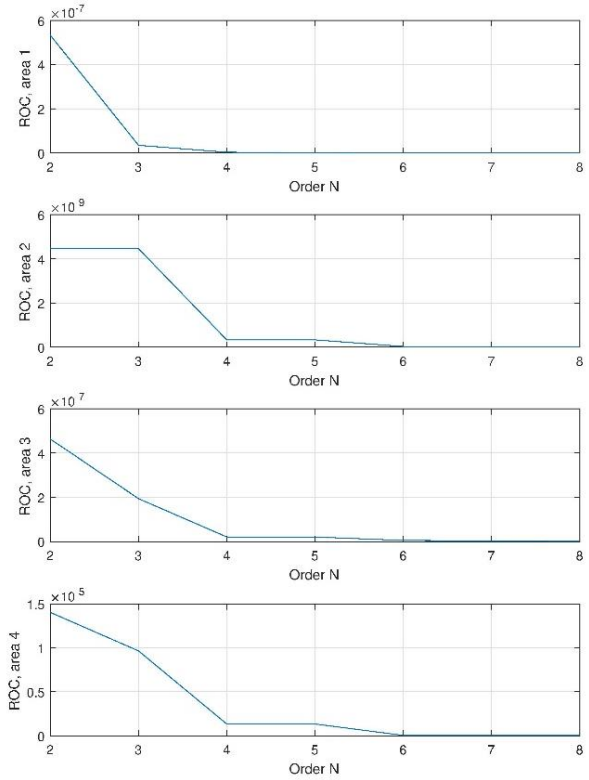


**Fig. 6.** The Rate of Convergence (38) for all areas and maximum orders $M = N = 8$

## 5. CONCLUSIONS

The main final conclusion from this paper is that the proposed, fully FO model of the distributed parameter system assures better accuracy in the sense of the MSE cost function than the model using fractional derivative only along the time. In addition, the good accuracy can be achieved for relatively low order of model.

The future work will cover deeper analysis of the convergence of the proposed model. Numerical results show, that the convergence depends not only on orders M and N but also on the location and size of area of measurement.

Another important issues are e.g. the positivity analysis as well as the use of a new fractional operators with nonsingular kernel: Atangana-Baleanu and Caputo-Fabrizio to modelling of the presented system.

Next, the use of thermal camera allows to collect many interesting data from different thermal processes, e.g. it allows to investigate thermal processes going in microcontroller system during its work. Such a process can be also described using FO approach and this is planned to describe using the proposed approach.

## REFERENCES

1. Podlubny I. Fractional Differential Equations San Diego: Academic Press; 1999.
2. Dzieliński A, Sierociuk D, Sarwas G. Some applications of fractional order calculus. Bulletin of the Polish Academy of Sciences, Technical Sciences. 2010.
3. Caponetto R, Dongola G, Fortuna L, Petra I. Fractional order systems: Modelling and Control Applications. University of California ed. Chua LO, editor. Berkeley: World Scientific Series on Nonlinear Science; 2010.
4. Das S. Functional Fractional Calculus for System Identification and Controls Berlin: Springer; 2010.
5. Gal CG, Warma M. Elliptic and parabolic equations with fractional diffusion and dynamic boundary conditions. Evolution Equations and Control Theory. 2016.
6. Popescu E. On the fractional Cauchy problem associated with a feller semigroup. Mathematical Reports. ; 2010.
7. Sierociuk D, Skovranek T, Macias M, Podlubny I. Diffusion process modelling by using fractional-order models. Applied Mathematics and Computation. 2015.
8. Gómez JF, Torres L, Escobar RF. Fractional derivatives with Mittag-Leffler kernel. Trends and applications in science and engineering Kacprzyk J, editor. Switzerland: Springer; 2019.
9. Boudaoui A, El hadj Moussa Y, Hammouch , Ullah S. A fractional-order model describing the dynamics of the novel coronavirus (covid-19) with nonsingular kernel. Chaos, Solitons and Fractals. 2021; 146(110859):111.
10. Muhammad Farman M, Akgül A, Askar S, Botmart T. Modelling and analysis of fractional order zika model. AIMS Mathematics. 2022.
11. Oprzędkiewicz K, Gawin E, Mitkowski W. Modeling heat distribution with the use of a non-integer order, state space model. International Journal of Applied Mathematics and Com-puter Science. 2016.
12. Oprzędkiewicz K, Gawin E, Mitkowski W. Parameter identification for non-integer order, state space models of heat plant. In MMAR 2016 : 21th international conference on Methods and Models in Automation and Robotics; 2016; Międzyzdroje, Poland. p. 184-188.
13. Oprzędkiewicz K, Stanisławski R, Gawin E, Mitkowski W. A new algorithm for a cfe approximated solution of a discrete-time non integer-order state equation. Bulletin of the Polish Academy of Sciences. Technical Sciences. 2017; 65(4):429-437.
14. Oprzędkiewicz K, Mitkowski W, Gawin E. An accuracy estimation for a non-integer order, discrete, state space model of heat transfer process. In Automation 2017 : innovations in automation, robotics and measurement techniques; 2017; Warsaw, Poland. p. 86-98.
15. Oprzędkiewicz K, Mitkowski W, Gawin E, Dziedzic K. The Caputo vs. Caputo-Fabrizio operators in modelling of heat transfer process. Bulletin of the Polish Academy of Sciences. Technical Sciences. 2018; 66(4):501-507.
16. Oprzędkiewicz K, Gawin E. The practical stability of the discrete, fractional order, state space model of the heat transfer process. Archives of Control Sciences. 2018.
17. Oprzędkiewicz K, Mitkowski W. A memory efficient non in-teger order discrete time state space model of a heat transfer process. International Journal of Applied Mathematics and Computer Science. 2018.
18. Oprzędkiewicz K. Non integer order, state space model of heat transfer process using Atangana-Baleanu operator. Bulletin of the Polish Academy of Sciences. Technical Sciences. 2020; 68(1):43-50.
19. Długosz M, Skruch P. The application of fractional-order models for thermal process modelling inside buildings. Journal of Building Physics. 2015; 1(1):1-13.
20. Ryms M, Tesch K, Lewandowski W. The use of thermal imaging camera to estimate velocity profiles based on tem-perature distribution in a free convection boundary layer. International Journal of Heat and Mass Transfer. 2021.
21. Khan H, Shah R, Kumam P, Arif M. Analytical solutions of fractional order heat and wave equations by the natural transform decomposition method. Entropy. 2019.
22. Olsen-Kettle L. Numerical solution of partial differential equa-tions Brisbane: The University of Queensland; 2011.
23. Al-Omari SK. A fractional Fourier integral operator and its extension to classes of function spaces. Advances in Difference Equations. 2018; 1(195):19.
24. Oprzędkiewicz K, Mitkowski W, Rosół M. Fractional order model of the two dimensional heat transfer process. Energies. 2021.
25. Kaczorek T. Singular fractional linear systems and electrical circuits. International Journal of Applied Mathematics and Computer Science. 2011.

26. Kaczorek T, Rogowski K. Fractional Linear Systems and Electrical Circuits Białystok: Publishing House of the Bialystok University of Technology; 2014.
27. Bandyopadhyay B, Kamal S. Solution, stability and realization of fractional order differential equation. In A Sliding Mode Approach, Lecture Notes in Electrical Engi-neering 317. Switzerland: Springer; 2015. p. 5590.
28. Wyrwas M, Mozyrska D, Girejko E. Comparison of h-difference fractional operators. In Mitkowski W, editor. Advances in the Theory and Applications of Non-integer Order Systems. Switzerland: Springer; 2013. p. 1-178.
29. Berger J, Gasparin S, Mazuroski W, Mende N. An effi-cient two-dimensional heat transfer model for building enve-lopes. An International Journal of Computation and Methodology, Numerical Heat Transfer, Part A: Applications. 2021; 79(3):163194.
30. Moitsheki RJ, Rowjee A. Steady heat transfer through a two-dimensional rectangular straight fin. Mathematical Problems in Engineering. 2011.
31. Yang L, Sun B, Sun X. Inversion of thermal conductivity in two-dimensional unsteady-state heat transfer system based on finite difference method and artificial bee colony. Applied Sciences. 2019.
32. Mitkowski W. Outline of Control Theory Kraków: Publishing House AGH; 2019.
33. Brzek M. Detection and localisation structural damage in selected geometric domains using spectral theory (in Polish). PhD thesis ed. Mitkowski W, editor. Kraków: AGH University of Science and Technology; 2019.
34. Michlin SG, Smolicki CL. Approximate methods for solving differential and integral equations (in Polish) Warszawa: PWN; 1970.

This paper was sponsored by AGH UST project no 16.16.120.773.

Krzysztof Oprzędkiewicz: https://orcid.org/0000-0002-8162-0011

Wojciech Mitkowski: https://orcid.org/0000-0001-5704-8329

Maciej Rosół: https://orcid.org/0000-0003-1176-7904